A 10-MHz GaN HEMT DC/DC Boost Converter for Power Amplifier Applications

Florent Gamand, Ming Dong Li, and Christophe Gaquière

***Abstract*—AlGaN/GaN HEMTs show low ON-state resistance and small gate capacitances, which makes them good candidates for switching applications. Up to now, their exploitations in dc/dc converters have been largely investigated in high power electronics but with switching frequencies under 1 MHz. In this brief, the potentialities of GaN HEMTs are investigated for high-speed dc/dc converters. To this aim, a 10-MHz GaN 16–34-V boost converter with above-90% efficiency is presented. Such converters are well suited for high-efficiency power amplifiers based on dynamic bias control for high peak-to-average-power-ratio applications.**

***Index Terms*—Converter, dc/dc, dynamic bias, GaN, HEMT, high efficiency.**

I. Introduction

Owing to their capability of managing high power levels, good linearity properties, and high transition frequency, GaN-based transistors have demonstrated excellent performances in microwave circuits, such as high-efficiency power amplifiers, low-noise amplifiers, and mixers. GaN HEMTs also show a low drain–source on-resistance, due to their high current density, and relatively small gate capacitances C_{GD} and C_{GS} as HEMTs are lateral devices. These characteristics make AlGaN/GaN HEMTs good candidates for switchlike applications. Their use in dc/dc converter circuit has been recently investigated by means of numerical analysis [1] or in demonstrator for very high power applications (up to 425 W), reaching efficiencies up to 97% [2], [3]. An example of a boost converter in GaN monolithic technology was also presented in [4]: Eighty-four-percent efficiency was here achieved for converting 10 V to 21 V, by means of a normally off AlGaN/GaN HEMT and a lateral field-effect rectifier. However, these converters were limited to a 1-MHz switching frequency, which leads to large sizes of passive components and a limited converter bandwidth. This is particularly important for targeting radio frequency (RF) applications like dynamic drain bias power amplifier. The dynamic drain bias can be adopted in high-efficiency systems to keep a high power-added efficiency (PAE) in the presence of important peak-to-average power ratio (PAPR) variations. A MOSFET-based buck dc/dc converter was used with a GaAs class-E amplifier in [5], obtaining the PAE to pass from 41.5% to 60%. In [6], a Cree CGH40025 GaN HEMT was used in a 60-MHz boost converter with up to 90% efficiency, but authors did not give any details about passive components used in the converter.

Manuscript received March 19, 2012; revised July 24, 2012; accepted October 18, 2012. Date of publication December 20, 2012; date of current version January 4, 2013. This work was supported by Centre National de la Recherche Scientifique. This brief was recommended by Associate Editor W.-H. Ki.

The authors are with the Institute of Electronics, Microelectronics and Nanotechnology, 62652 Villeneuve d'Ascq, France (e-mail: florent.gamand@ed.univ-lille1.fr; ming-dong.li@iemn.univ-lille1.fr; christophe.gaquiere@iemn.univ-lille1.fr).

Color versions of one or more of the figures in this brief are available online at http://ieeexplore.ieee.org.

Digital Object Identifier 10.1109/TCSII.2012.2228397

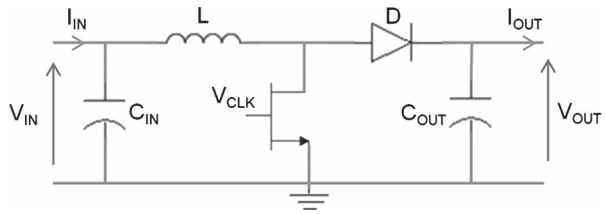

Fig. 1. Circuit schematic of the boost dc/dc converter.

The target of this brief is to investigate the possibility of designing a high-speed 10-MHz dc/dc converter for RF power applications by using the same HEMT technology as in RF power amplifiers and standard commercial passive components. To this aim, a simple boost converter was designed to convert the 16-V input voltage to an output voltage varying between 17 and 40 V, with an output power up to 20 W; these voltage and power ranges are compatible with typical drain bias supply requirements in GaN amplifiers. Measurements at 5- and 20-MHz switching frequencies as well as high temperature measurements have also been performed to demonstrate the potentialities of this technology.

II. DC/DC Converter

A. Converter Description and Theory

A typical boost configuration is chosen for this study. The circuit schematic is shown in Fig. 1. The transistor is controlled by a gate–source voltage pulse swinging between pinchoff and open-channel values. The duty cycle D of the gate signal (V_{CLK}) controls the converter output voltage, ideally according to the following relation:

$$V_{\mathrm{OUT}} = V_{\mathrm{IN}} \times \frac{1}{1-D}. \tag{1}$$

A dc/dc converter is asked to provide high efficiency, at least greater than 80%. To satisfy this requirement, the power losses in the circuits must be particularly reduced. Two kinds of losses can be distinguished depending on whether they relate to conduction or switching phenomena.

The conduction losses include power dissipations on the inductance L, on the transistor, and on the diode. The switching

TABLE I
CONDUCTION LOSSES

Losses in the inductor	$P_L = R_L \cdot I_{IN}^2$
Losses in the transistor	$P_T = R_{DS\_ON} \cdot I_{IN}^2 \cdot D$
Losses in the diode	$P_D = \left(R_D \cdot I_{IN}^2 + V_F \cdot I_{IN}\right) \cdot (1 - D)$

TABLE II
SWITCHING LOSSES

ON-OFF switching losses	$P_f = 0.5 \cdot V_{OUT} \cdot I_{IN} \cdot \frac{T_f}{T_0}$
OFF-ON switching losses	$P_r = 0.5 \cdot V_{OUT} \cdot I_{IN} \cdot \frac{T_r}{T_0}$

losses are due to the noninstantaneous commutation times. They depend on the switching fall and rise times, which are mainly determined by the gate–drain and gate–source capacitances of the transistor and the junction capacitance of the diode.

Simplified expressions of these losses are given in Tables I and II, respectively. R_L is the dc inductor resistance, $R_{\mathrm{DS\_ON}}$ is the transistor on-resistance, R_D is the diode series resistance, and V_F is the diode forward voltage. T_f and T_r are the fall and rise times of the transistor drain current, respectively, while T_0 is the period of the control signal. The approximate expression for the converter efficiency is given by

$$\eta \approx \frac{P_{\mathrm{OUT}}}{P_{\mathrm{OUT}} + P_L + P_T + P_D + P_f + P_r} \tag{2}$$

where P_{OUT} is the output power of the converter. By replacing the different power losses in (1) with the expressions reported in Tables I and II, the efficiency can be written as follows:

$$\eta = \frac{1}{A} \tag{3}$$

$$A = 1 + \frac{R_L + R_{\mathrm{DS\_ON}} * D + R_D * (1 - D)}{V_{\mathrm{OUT}}/(I_{\mathrm{OUT}} * m^2)} + \frac{V_F}{V_{\mathrm{IN}}} * (1 - D) + m * \frac{T_r + T_f}{2 * T_0} \tag{4}$$

where m is the conversion ratio $V_{\mathrm{OUT}}/V_{\mathrm{IN}}$. From (3) and (4), the importance of having low parasitic resistances for each element of the circuit and fast switching time for the transistor and the Schottky diode is evident.

B. DC/DC Boost Converter Demonstrator

The demonstrator is a hybrid circuit based on an FR4 1.5-mm substrate where passive surface-mount components are soldered; the GaN switch is mounted on a copper baseplate for heat dissipation.

The switching device is a GaN-on-Si HEMT from Nitronex designed for RF applications. The device has the following features: The on-resistance is 1.2 Ω, the gate threshold voltage is −1.9 V, the maximum drain current is 3 A at $V_{\mathrm{GS}} = 1$ V, and the static gate–drain breakdown voltage is around 100 V. The current cutoff frequency is 6 GHz.

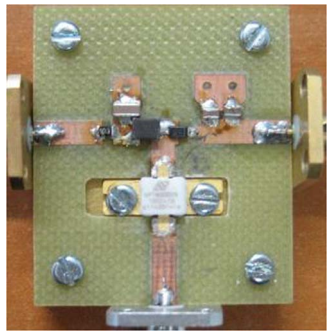

Fig. 2. Photograph of the proposed boost dc/dc converter.

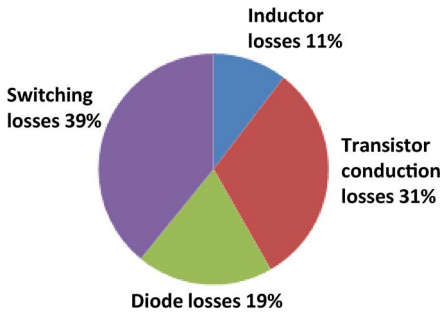

Fig. 3. Distribution of power losses in the boost dc/dc converter with $V_{\mathrm{IN}} = 16$ V, $V_{\mathrm{OUT}} = 34$ V, and $P_{\mathrm{OUT}} = 15$ W.

The input decoupling capacitor C_{IN} is 0.47 μF; the output capacitor C_{OUT} is 47 nF. The inductor choice is quite challenging in this application as it results from the tradeoff between size, self-resonant frequency (FSR), and current handling. In this prototype, the chosen inductor is 3.3 μH with a 0.15-Ω dc resistance, 140-MHz FSR, and 1.4-A rated current; a 1-μH inductor of the same type has also been tested. Finally, the diode is a Schottky rectifier with a 0.5-V forward voltage, a 0.14-Ω serial resistance, and a 150-pF zero bias capacitor. The average forward current is 1 A and the reverse recovery time is less than 10 ns. The typical load is a 25-W 75-Ω noninductive resistance mounted on a copper heat sink. The converter circuit is shown in Fig. 2; the load resistance and the copper heat sink are not on the picture. Fig. 3 shows an estimation of the loss distribution according to the equations of Tables I and II for selected components and a 16–34-V 10-MHz converter; the major contributions to total losses are the switching losses (39%) and transistor conduction losses (31%), showing the key role of the switching device in the dc/dc converter.

III. MEASUREMENT RESULTS

For each measurement, the transistor gate voltage is controlled by a pulse generator providing a 2-ns switching time corresponding to the switching performance of the used GaN HEMT and the input voltage is provided by a classical laboratory dc power supply. The waveforms are measured with a 500-MHz-bandwidth oscilloscope.

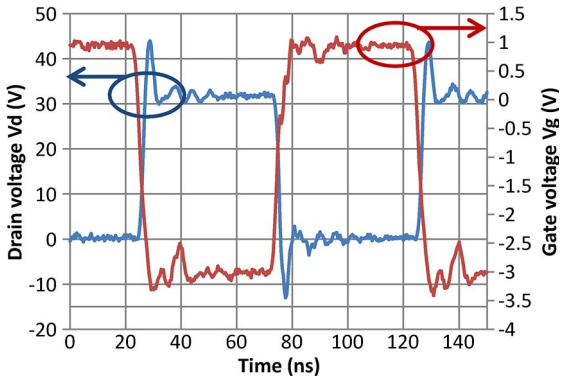

Fig. 4. Measured waveforms of the switching device gate and drain voltages at 10 MHz. Input voltage is 16 V, load resistance is 75 Ω, and duty cycle is 0.5.

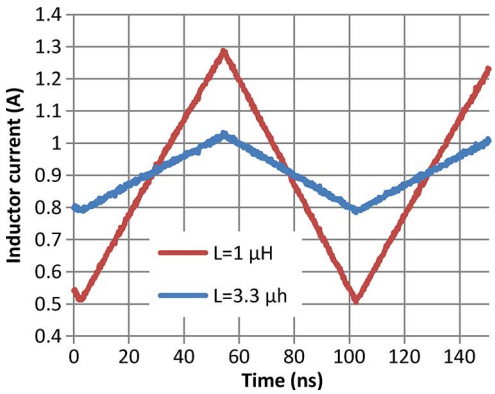

Fig. 5. Measured waveforms of the inductor current at 10 MHz for $L = 1$ and 3.3 μH. Input voltage is 16 V, load resistance is 75 Ω, and duty cycle is 0.5.

A. Waveform Measurement at 10 MHz

The drain and gate voltages for a 75-Ω load resistance and a duty cycle of 0.5 are shown in Fig. 4; the switching frequency is 10 MHz. The transistor gate voltage switches between -3 and 1 V, while the drain voltage switches between $I_{\rm IN} * R_{\rm DS\_ON}$ and $V_{\rm OUT} + V_F$, which are close to 0 and 32 V here. The measured switching time for the drain voltage is 3 ns.

The current across the inductor is measured with a shunt resistance and is plotted in Fig. 5, the duty cycle is 0.5, and the load resistance is 75 Ω. Two different inductors have been used, 1 and 3.3 μH. The average current is 0.9 A, and the ripple is 0.2 A (22%) for the 3.3-μH inductor and 0.8 A (89%) for the 1-μH inductor. Even with the 1-μH inductor, the peak current (1.3 A) remains below the maximum rated current in the inductor (1.4 A); choosing a smaller inductance value allows increasing the slew rate of the converter, as shown in Fig. 6. The slew rate of the converter increases from 10 to 18 V/μs; the overshoot is also reduced.

B. Efficiency Measurements and Simulations

Measured and simulated efficiencies for a 16-V input at varying output power and corresponding voltages are plotted in Fig. 7. Transient simulations have been performed using the Advanced Design System commercial software, the transistor model was provided by Nitronex, and the diode was modeled through dc and impedance measurements. The measured ef-

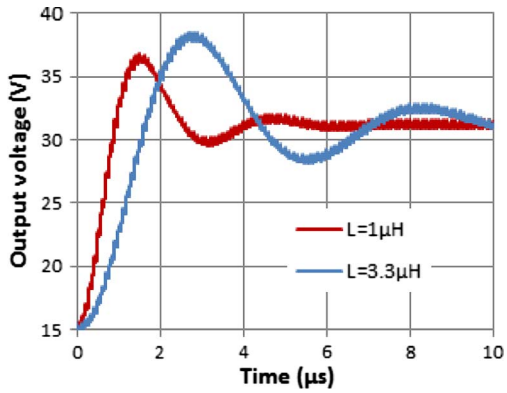

Fig. 6. Measured waveforms of the output voltage of the converter at 10 MHz for $L = 1$ and 3.3 μH. Input voltage is 16 V, load resistance is 75 Ω, and duty cycle is 0.5.

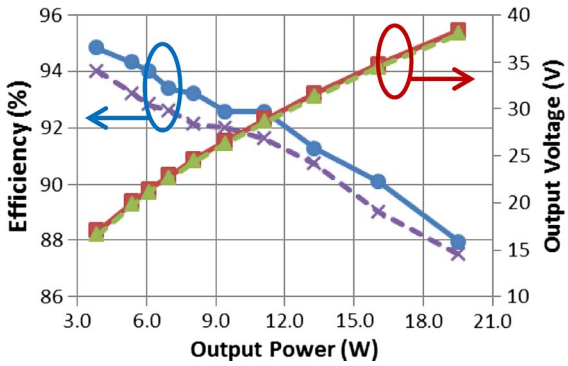

Fig. 7. (Straight line) Measured and (dashed line) simulated converter efficiencies at varying output power and corresponding values of the output voltage. The switching frequency is 10 MHz and the input voltage is 16 V.

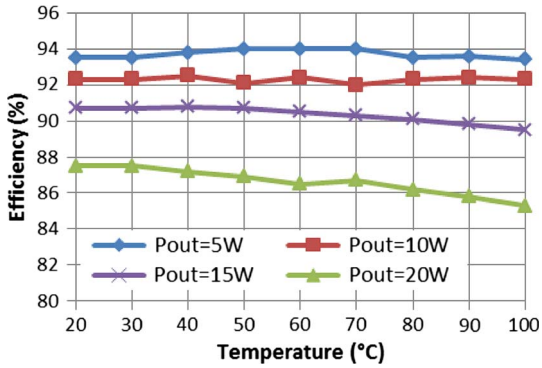

Fig. 8. Measured boost converter efficiency at varying temperatures and different values of the output power. The switching frequency is 10 MHz and the input voltage is 16 V.

ficiency is above 90% for output voltages and powers up to 34 V and 16 W, respectively; at 38 V and a 20-W output power corresponding to a 0.6 duty cycle, efficiency is still 88%. The efficiency decrease with the output voltage is mainly due to the switching losses proportional to $V_{\rm OUT}$, as shown in Table I. It is worth noting that there is a good agreement between measure and simulation, with 1.5% and 0.2-V maximum gap for efficiency and output voltage, respectively.

Fig. 8 shows the efficiency evolution with an operating temperature up to 100 °C for output powers between 5 and 20 W; the maximum efficiency decrease is 2% at 20-W output power

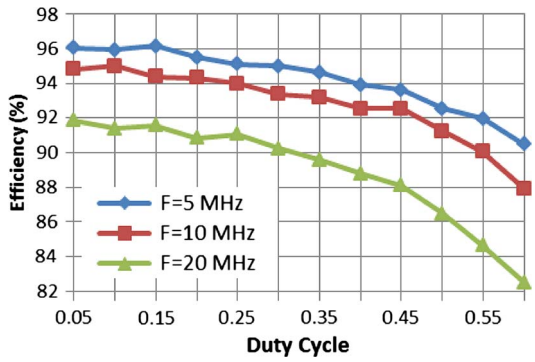

Fig. 9. Measured converter efficiency at varying duty cycles, for switching frequencies of 5, 10, and 20 MHz. The input voltage is 16 V.

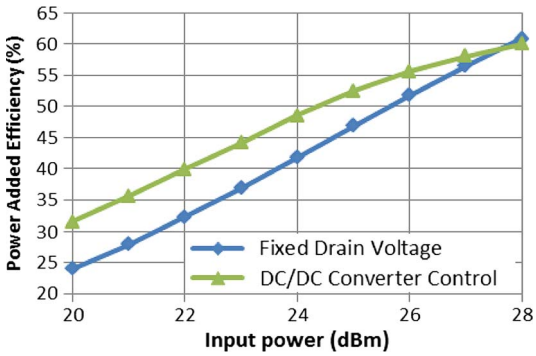

Fig. 10. Comparison of estimated PAE with and without a dynamic bias drain polarization.

and 100 °C; otherwise, the converter efficiency is stable with temperature, showing GaN good performances at relatively high temperature (no system of cooling used).

As plotted in Fig. 9, the efficiency decreases by 3%–5%, while the switching frequency is set to 20 MHz instead of 10 MHz because the rise and fall times are more significant as the frequency increases. However, efficiency remains above 82% for the duty cycle ranging from 0 to 0.6.

An estimation of the PAE for a simulated 2-GHz GaN power amplifier using the same transistor as the DC/DC converter is shown in Fig. 10. The PAE is improved by 7% by the dynamic drain biasing (taking into account measured converter efficiencies) for input power variation between 20 and 24 dBm; the PAE is improved until a 28-dBm input power. This 8-dB power dynamic is compatible with PAPR of modulation like Long Term Evolution (PAPR = 6 dB) or Worldwide Interoperability for Microwave Access (PAPR = 8 dB). Detailed implementation and measurements of the amplifier will be reported in the next presentation.

IV. Conclusion

A 10-MHz boost dc/dc converter has been designed in order to investigate GaN potentialities for high-speed converters dedicated to RF applications, such as dynamic bias amplifiers. Measurement results are presented for a wide range of output powers, showing efficiencies above 90%. The converter also exhibits a good behavior at temperatures up to 100 °C, which is better than most Si-based converters. Frequency measurements show promising results for reaching higher switching frequencies with newer GaN devices, thus decreasing component size and increasing converter bandwidth needed for RF applications.

Acknowledgment

The authors would like to thank EUREKA PANAMA "Power Amplifiers and Antennas for Mobile Applications" contract for their financial support.

References

[1] Y. Gao and A. Q. Huang, "Feasibility study of AlGaN/GaN HEMT for multimegahertz DC/DC converter applications," in *Proc. IEEE IPEMC*, 2006, vol. 2, pp. 1–3.

[2] Y. Wu, M. Jacob-Mitos, M. L. Moore, and S. Heikman, "A 97.8% efficient GaN HEMT boost converter with 300-W output power at 1 MHz," *IEEE Electron Device Lett.*, vol. 29, no. 8, pp. 824–826, Aug. 2008.

[3] J. Das, J. Everts, J. Van Den Keybus, M. Van Hove, D. Visalli, P. Srivastava, D. Marcon, K. Cheng, M. Leys, S. Decoutere, J. Driesen, and G. Borghs, "A 96% efficient high-frequency DC–DC converter using E-mode GaN DHFETs on Si," *IEEE Electron Device Lett.*, vol. 32, no. 10, pp. 1370–1372, Oct. 2011.

[4] W. Chen, K.-Y. Wong, and K. J. Chen, "Single-chip boost converter using monolithically integrated AlGaN/GaN lateral field-effect rectifier and normally off HEMT," *IEEE Electron Device Lett.*, vol. 30, no. 5, pp. 430–432, May 2009.

[5] N. Wang, V. Yousefzadeh, D. Maksimović, S. Pajić, and Z. B. Popović, "60% efficient 10-GHz power amplifier with dynamic drain bias control," *IEEE Trans. Microw. Theory Tech.*, vol. 52, no. 3, pp. 1077–1081, Mar. 2004.

[6] N. Le Gallou, D. Sardin, C. Delepaut, M. Campovecchio, and S. Rochette, "Over 10-MHz bandwidth envelope-tracking DC/DC converter for flexible high power GaN amplifiers," in *Proc. IEEE MTT-S Int.*, Jun. 2011, pp. 1–4.